Fermi National Accelerator Laboratory

FERMILAB-Conf-98/165

Main Injector Synchronous Timing System

Willem Blokland and James Steimel

Fermi National Accelerator Laboratory
P.O. Box 500, Batavia, Illinois 60510

February 1999

Published Proceedings of the *Beam Instrumentation Workshop 98*,
SLAC, Stanford, California, May 4-7, 1998

Operated by Universities Research Association Inc. under Contract No. DE-AC02-76CH03000 with the United States Department of Energy

Main Injector Synchronous Timing System

Willem Blokland and James Steimel

Fermi National Accelerator Laboratory,
Batavia, Illinois 60510

The Synchronous Timing System is designed to provide sub-nanosecond timing to instrumentation during the acceleration of particles in the Main Injector. Increased energy of the beam particles leads to a small but significant increase in speed, reducing the time it takes to complete a full turn of the ring by 61 nanoseconds (or more than 3 RF buckets). In contrast, the reference signal, used to trigger instrumentation and transmitted over a cable, has a constant group delay. This difference leads to a phase slip during the ramp and prevents instrumentation such as dampers from properly operating without additional measures. The Synchronous Timing System corrects for this phase slip as well as signal propagation time changes due to temperature variations. A module at the LLRF system uses a 1.2 Gbit/s G-Link chip to transmit the RF clock and digital data (e.g. the current frequency) over a single mode fiber around the ring. Fiber optic couplers at service buildings split off part of this signal for a local module which reconstructs a synchronous beam reference signal. This paper describes the background, design, and expected performance of the Synchronous Timing System.

INTRODUCTION

The Main Injector ramps from 52.812 MHz to 53.104 MHz during the acceleration from 8 GeV to 150 GeV while increasing the speed of the particles. Given that there are 588 buckets in the Main Injector, a single turn goes from 11134 ns to 11073 ns, a difference of 61 ns. In contrast, the reference signal, transmitted over a cable, has a constant group delay. This difference leads to a phase slip that, at MI-30 or halfway around the Main Injector, is the group delay, 12 μs for a single-mode fiber, multiplied by the frequency sweep, 300 kHz, or more than 3 RF cycles. That is unacceptable for a damper system or a synchronously sampling beam position system.

The idea behind the Synchronous Timing System (STS) is to provide instrumentation around the Main Injector with a trigger synchronous to a particular bunch of the beam even during acceleration. Previous work done at Fermilab on obtaining a beam synchronous trigger is described in [1]. However, this system used a frequency counter on the RF signal to determine the frequency. The STS will transmit not only the RF but also a digitally encoded frequency value to simplify the design of the local receiver. A different approach to obtain a synchronous phase is to add a delay to the LLRF feedback loop that is equal to the cable delay from the LLRF to the local receiver. However, for the Main Injector LLRF such a delay would complicate the LLRF system and might even lead to instabilities.

An added complication is the temperature dependency of the signal carrying medium. For example, for a single-mode fiber this can be up to 30 ps/Ckm. With a 10 ℃ variance in duct temperature and a cable length of 5 km, the total time differs about 1.5 ns. That is enough of a variation that the Synchronous Timing System needs temperature compensation. The STS design aims to provide a synchronous trigger with timing noise of around a 100 ps RMS. This will satisfy the requirements for instrumentation like dampers or synchronous beam position sampling systems and support beam instability studies.

The following sections in this paper describe the reconstruction of the phase, the signal distribution infrastructure, and the design of the receiver and transmitter boards.

SYNCHRONOUS TIMING

The STS must correct the phase to account for the difference in travel times between the reference signal and the particle speed as well as the variations in the group delay due to temperature changes. This chapter first analyzes the phase as a function of frequency (RF) followed by an analysis of the phase as a function of temperature.

Phase as a Function of Frequency

The LLRF is trying to keep the particles at the same phase for each turn no matter what the frequency, as the number of buckets remains the same. This is true for any location around the ring. As the frequency increases, the phase of the reference signal shifts as more cycles fit within the same cable length. Therefore the local receiver must "unwind" the phase of the RF signal to construct a synchronous phase. This is done by subtracting a delta phase that is the product of the change in frequency and the time-of-flight of the RF signal. In addition, a phase intercept is added to align the phase of the reconstructed RF with the phase of a detector:

$$\begin{gathered}\varphi_{sync} = \varphi_{RF} - \Delta\varphi + \varphi_{intercept} \\ \Delta\varphi = \Delta\omega \cdot \tau\end{gathered} \tag{1}$$

with $\Delta\omega = \omega - \omega_{base}$, ω_{base} = radian frequency at beginning of cycle, τ = time-of-flight of RF, and $\varphi_{intercept}$ = phase intercept.

Phase as a Function of Temperature

The temperature dependency is modeled as an extra delay in the cable as a function of temperature:

$$\Delta\tau = \left(v(T_0) - v(T_1)\right) \cdot l \qquad (2)$$

with l = length of cable, T_i= temperature at time i, and $v(T_i)$ = signal speed at T_i.

The $\Delta\tau$ will be measured indirectly by comparing the phase of the RF signal generated by the transmitter board and the phase of the RF signal received after it has gone around the ring. The receiver for this signal will be on the same board as the transmitter. The phase shift due to the $\Delta\tau$ is:

$$\Delta\varphi_{temp} = \omega \cdot \Delta\tau \qquad (3)$$

Assuming that the distribution of the temperature dependent phase shift is linear along the signal path then the local phase shift is:

$$\Delta\varphi_{temp}^{local} = \Delta\varphi_{temp}^{total} \cdot \frac{\tau^{local}}{\tau^{total}} \qquad (4)$$

with the value of a variable at an arbitrary location around the ring indicated by the superscript *local* and the location back at the LLRF after a full turn indicated by the superscript *total*.

The change due to temperature variation is very slow compared to the change due to frequency sweeping. The cable ducts are buried 4 to 7 feet and should change only about 10 °C over the seasons. Fast changes between the generated and received phase will be regarded as errors that should be diagnosed. Even if the temperature varied by 1 °C over a day this would only be a change of 0.1 ps per minute.

Reconstructed and Temperature Compensated Phase

The compensating phase shift to be locally added to the RF signal is the sum of the frequency phase slip and temperature compensation:

$$\Delta\varphi^{local} = \Delta\omega \cdot \tau^{local} + \Delta\varphi_{temp}^{total} \cdot \frac{\tau^{local}}{\tau^{total}} \qquad (5)$$

This can be rewritten so that only the correction term $\Delta\omega + \Delta\varphi_{temp}^{total} / \tau^{total}$ must be transmitted:

$$\Delta\varphi^{local} = \left(\Delta\omega + \frac{\Delta\varphi_{temp}^{total}}{\tau^{total}} \right) \cdot \tau^{local} \qquad (6)$$

SIGNAL DISTRIBUTION

The distribution of the signal from the transmitter to the receivers is depicted in figure 1. The LLRF system provides the transmitter with a Voltage Controlled Oscillator (VCO) synchronized strobe and the required digital information. We choose single mode fiber as the medium because of its low cost, low attenuation, and high bandwidth. The low cost, $1 per foot per 24 fibers, gives it a price advantage over copper cables especially counting the number of channels per cable. The low attenuation, 0.35 dB/km, makes it possible to passively split off a part of the signal at each of the 10 service buildings while avoiding the use of amplifiers and associated noise. Figure 2 depicts the loss calculation and includes losses due to connectors, splitters, and 5 km of cable. The high bandwidth makes it possible to use the G-Link chip from Hewlett Packard [2] which supports a stream up to 1.2 Gbit/s. The STS will use the RF (53 MHz) as a clock and the 20 bits per clock cycle are used to carry the digitally encoded information. Finisar Optical modules [3] convert the G-Link signal to 1310 nm light waves and back. The STS will have for redundancy reasons two fibers with an active signal and a third fiber prepared for immediate use. The remaining 21 fibers are for future use.

The transmitters and receivers are VXI modules that, through the slot 0 processor, communicate with consoles using Fermilab's Accelerator Control Network (ACNET) protocol. This link is used for initialization, diagnostics, and calibration purposes.

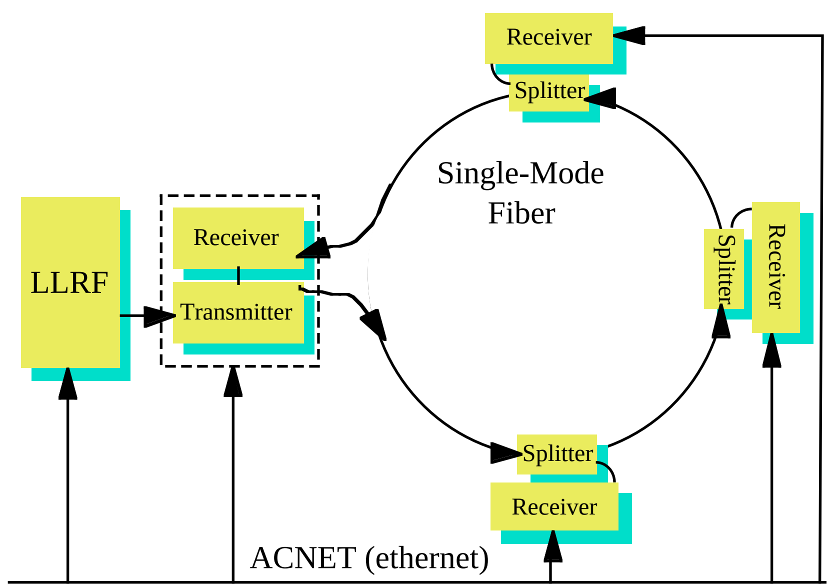

FIGURE 1. The signal distribution.

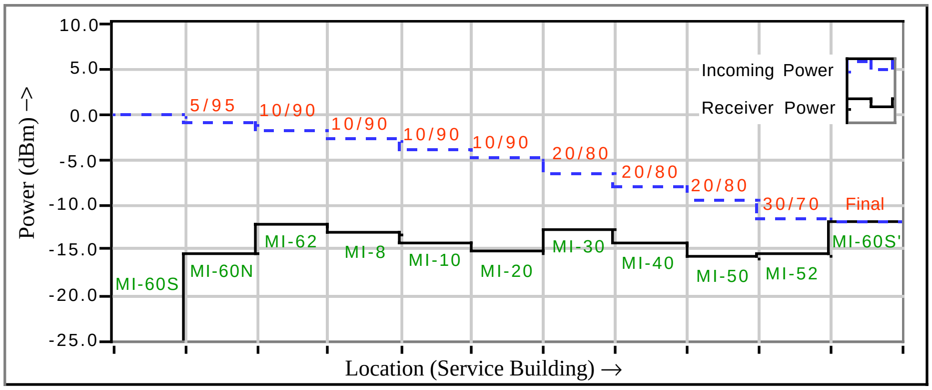

FIGURE 2. The passive splitting of a signal at each of the 10 service buildings. The top numbers indicate the splitter ratio while the top (dotted) line is the optical power in the incoming fiber to the service building. The lower (solid) line is the optical power to the receivers at each location with the name of the service building below the solid line. This calculation assumes a 1 dBm transmitter with a minimum receiver power requirement of -16 dBm.

RECEIVER AND TRANSMITTER DESIGN.

Besides correcting the phase, the STS must be able to identify a particular bunch or otherwise a damper would not know which bunch to kick. A marker reset is generated by the LLRF on injection of beam into the Main Injector. The transmitter sends this marker to the receivers which then reset a local bucket counter. This counter counts each cycle (read bucket) of the synchronized RF and resets when all 588 buckets passed by, thus always providing the same counter value for the same bucket.

Resolution Considerations

The maximum frequency change between updates, 10 µs, will be 20 Hz in the Main Injector, given the 2 MHz/s slew rate. This corresponds to about a 10 ps peak to peak jitter at the maximum cable delay of 25 µs.

The G-Link chip can transmit 20 bits per frame at a frame rate of 53 MHz. As the STS must transmit different messages, 4 bits are used to identify the type of message. This leaves 16 bits to describe the frequency sweep. Given a range of 500 kHz, (300 kHz is the current sweep range, 200 kHz extra range), the 16 bit word has a resolution of 500 kHz/65536 or 7.6 Hz. With the delay of 25 µs this results in a jitter of 4 ps peak to peak. These (uniform white noise) quantization errors lead to a RMS noise of $\sqrt{((10^2 + 4^2)/12)} \approx 3$ ps. This is small compared to RMS noise from the G-Link chip, about 42 ps. We do expect contributions from other parts of the electronics but not so high that we will come above a 100 ps RMS noise total.

The RF signal from the LLRF, however, is not perfect. It is estimated that, depending on what cycle is running in the Main Injector, there is about a 100 ps of RMS noise in this signal that is relevant to a damper system. Improvements on the quality of the RF signal will be for a future project.

The Receiver

The design of the receiver is shown in figure 3. The STS signal comes in over the fiber and is converted into a parallel stream of 20 bits data frame with a 53 MHz strobe by the Optical Receiver consisting of a Finisar FRM 1310 and a G-Link module. Diagnostic data from the G-Link and Finisar module are accessible over the VXI interface. The strobe is used as a clock to the Phase Shifter and Phase Calculation. The frame is decoded on an Altera chip into the correction term of equation (6) or a marker reset event. The Phase Calculation performs the multiplication in equation (6) and adds two more phase offsets. One is the intercept phase, $\varphi_{intercept}$, to align the synchronous phase with the phase of a beam pickup. The other is a phase from a local analog signal that could be part of a PLL on a beam signal to help improve the synchronous phase. ACNET can access the local intercept phase, $\varphi_{intercept}$, and time-of-flight ,τ_{local}, values over the VXI interface for calibration setup. The Phase Shifter is an I&Q modulator circuit. The Altera chip implements the sine and cosine functions of the corrected phase. These signals are converted to analog to be multiplied by the quadrature components of the strobe signal, summed together and bandpass filtered. The resulting signal is used to pulse the counter of the Pattern Generator and used as the synchronous RF output signal. The Pattern Generator contains a single byte wide memory bank with one byte for each bucket and one bit for each of the 8 output Triggers. The Pattern Generator's memory is set using ACNET. To allow easy calibration and diagnostics, the correction term, the calculated shift, $\Delta\varphi$, and the local signal are available through the Multiplexer (MUX) unit and the D/A converter as a analog signal or through the VXI interface as a digital value.

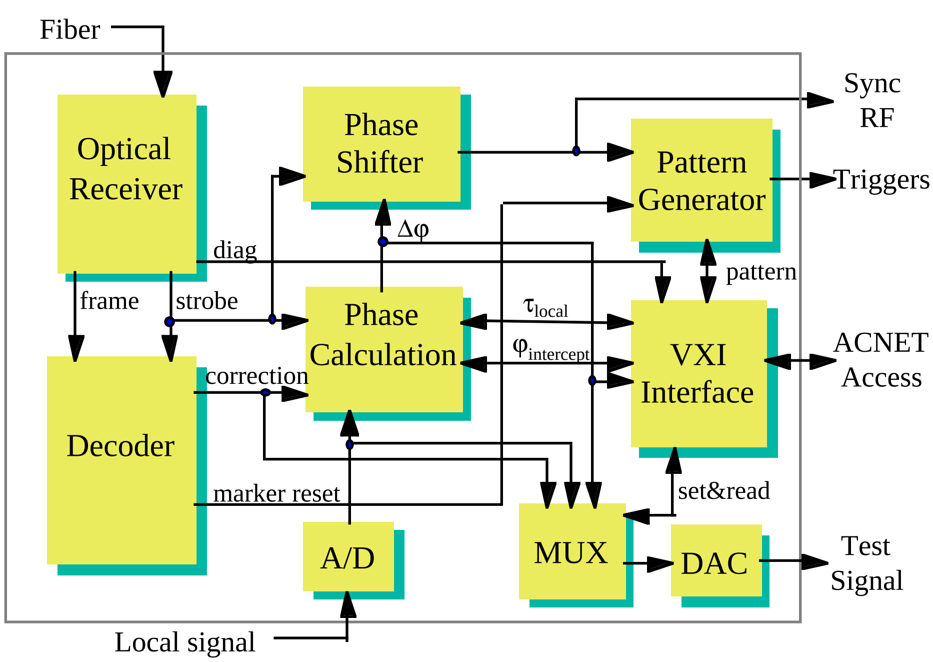

FIGURE 3. Diagram of the receiver.

The Transmitter

The transmitter module, see figure 4, provides the optical signal used by the receiver modules. This signal is synchronized with the RF by the VCO of the LLRF and contains information on the frequency value, the change in fiber delay due to temperature, and the beam marker reset. The module is located close to the Main Injector LLRF system, and it contains the same DSP, an Analog Devices' SHARC, as the LLRF system [4]. Using the same DSP simplifies communication between the two systems and also maximizes data transfer speed. The LLRF DSP transfers frequency information to the transmitter DSP through a fast Link Port.

Each transmitter module contains all the components of a receiver module except the pattern generator and the A/D converter. This receiver decodes the transmitter signal which has traveled the full circumference of the ring. The Phase Detector of the transmitter compares the synchronized output of the receiver module with the RF input of the transmitter module. Errors are accumulated and used to calculate the phase shift due to temperature, $\Delta\varphi_{temp}$. The Phase Calculation, implemented on the DSP, uses the digital frequency from the LLRF f_{LLRF}, the phase shift $\Delta\varphi_{temp}$, and the time-of-flight τ^{total}, to calculate the correction term. The marker reset is sent directly to the encoder to avoid processor delays which might disrupt the single bucket precision of the signal. Access to the receiver and the τ^{total} value is handled by ACNET.

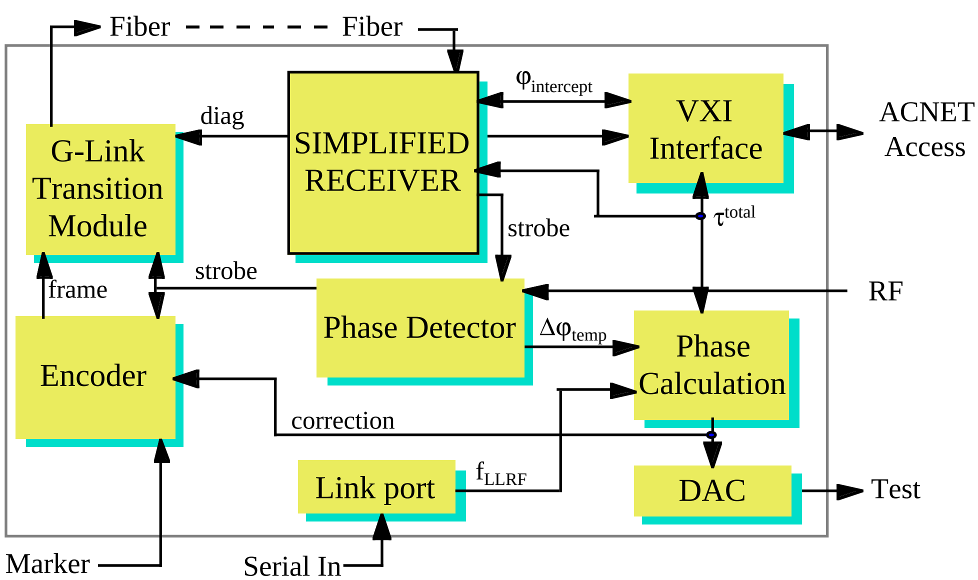

FIGURE 4. Block Diagram of transmitter.

CONCLUSIONS

We have designed a timing system that delivers a trigger synchronous to the beam during acceleration. The infrastructure has been installed and work to layout the transmitter and receiver boards is in progress. We expect that the noise added by the STS to the synchronous trigger will be less than 100 ps RMS. As the RF signal has about a 100 ps RMS noise to it, the total noise is estimated around 140 ps. This can be improved locally by locking to a signal from a beam pickup for those applications that don't require first turn sampling. In the future we hope to improve RF signal from the LLRF to further reduce the noise in the synchronous trigger.

ACKNOWLEDGEMENTS

Many thanks go to Brian Chase, Jim Crisp, and Keith Meisner for ideas and recommendations on the design issues.

REFERENCES

[1] Steimel, J., "Trigger Delay Compensation for Beam Synchronous Sampling," 7th Beam Instrumentation Workshop (BIW 96), Argonne, IL, May 1996, pp 476-482.

[2] Yen, C.S. et al., "G-Link: A Chipset for Gigabit-Rate Data Communication," *Hewlett-Packard Journal*, **43**(3), 103-116, (October 1992).

[3] "FTM/FRM-8510 Low Cost Gigabit Optical Transmitter/Receiver," Finisar Corporation, Mountain View, California.

[4] Chase, B. et al., "Current DSP Applications in Accelerator Instrumentation and RF," presented at the International Conference on Accelerator and Large Experimental Physics Control Systems (ICALEPCS'97), Beijing, China, Nov. 3-7, 1997.